Comparative Analysis of Ultra-Wideband and Mobile Laser Scanning Systems for Mapping Forest Trees under A Forest Canopy

Zuoya Liu[1], Harri Kaartinen[1], Teemu Hakala[1], Heikki Hyyti[1], Antero Kukko[1,2], Juha Hyyppa[1,2], Ruizhi Chen[3]

[1] Department of Remote Sensing and Photogrammetry, Finnish Geospatial Research Institute, Vuorimiehentie 5, 02150, Espoo, Finland – (zuoya.liu, harri.kaartinen, teemu.hakala, heikki.hyyti, antero.kukko, juha.hyyppa)@nls.fi
[2] Department of Built Environment, School of Engineering, Aalto University, P.O. Box 11000, FI-00076, Aalto, Finland
[3] School of Data Science, The Chinese University of Hong Kong, Shenzhen, China - chenruizhi@cuhk.edu.cn

Keywords: Ultra-wideband, Mobile Laser Scanning System, Distance Measurement, Forest Survey and Management, Tree map.

Abstract

In this paper, we present an ultra-wideband (UWB)-based method for mapping forest trees under a forest canopy and compare its precision with that of three commercial mobile laser scanning systems (MLS): Zeb Horizon (GeoSLAM, UK), Hovermap (Emesent, Australia), and Deep Forestry (Deep Forestry, Sweden). The proposed method is simple to implement in forest environments, requiring reduced human efforts. The comparison was based on real-world datasets collected in a boreal forest in Finland, covering an area of approximately 50 m × 110 m, with tree locations obtained from a high-density airborne laser scanning (ALS) system as a reference. To our best knowledge, this is the first study to compare UWB and MLS for mapping forest trees in the literature. The experimental results show that the proposed method can accurately measure tree stem locations under the forest canopy with a root-mean-square-error (RMSE) of 14.44 cm and a mean-absolute-error (MAE) of 12.39 cm, providing accuracy comparable to that of the three tested MLSs. Therefore, the proposed method is sufficient for forest surveying and management.

1. Introduction

Accurately positioning trees in a forest environment is critical for forest surveying and management, such as collecting precise forest inventory data. To obtain more accurate information on the quality, quantity, and changes in the growing stock of the forests, it is necessary to accurately measure the location of each tree with submeter-level or even centimeter-level accuracy (Liang et al., 2018). Additionally, studies have shown that highly accurate tree maps are also essential for making future individual-tree-level harvesting plans, advancing forest automation, and enhancing the economic value extracted from the forest (Muhojoki et al., 2024).

Currently, tree location data is still mainly collected through traditional field measurements, which are costly and laborious. To address this, various tools and techniques based on data and image processing have been developed, reducing human effort compared to traditional methods. These include the use of Global Navigation Satellite System (GNSS) (Edson and Wing, 2012), ultra-wideband (UWB) (Pekka Savolainen, 2017) and mobile laser scanning systems (MLS) (Holopainen et al., 2013), etc.

Among them, MLS, which integrates GNSS positioning systems, inertial measurement units (IMU), and data collection sensors, is the most commonly used method for mapping forest trees under forest canopies (Liang et al., 2022). MLS can avoid GNSS signal obstruction caused by the forest canopies, efficiently model the surrounding forest environments in 3D, and then precisely extract tree stem locations using advanced algorithms (Hyyppä et al., 2020a). However, MLS faces challenges in maintaining accurate long-term measurements due to the IMU drifts and issues with Simultaneous Localization and Mapping (SLAM), which is used to obtain continuous localization data of the MLS during the measurement. These drifts worsen over time and increase with the increase of the trajectory, especially without correction sources such as GNSS data, which is a common behavior in SLAM systems (Kukko et al., 2017). Moreover, tree branches and trunks obstructing the laser pulses pose another significant challenge for MLS working under forest canopies, leading to directional-scanning bias and occlusion in results (Stovall et al., 2023). For example, in forests with high tree density, scanning from multiple positions is often required to accurately map all trees in the environment. Furthermore, MLS systems are generally expensive due to the integration of advanced sensors.

UWB can be used not only for communications but also for real-time location estimation with decimetre-level or centimetre-level accuracy by measuring "time-of-flight (ToF)" of the pulse signals with nanosecond-level resolution and thus the distance between the transmitter and the receiver. While UWB is commonly used for locating mobile devices in indoor environments, where line-of-sight (LoS) propagation is often ideal, it has also been explored for forest applications. In (Pekka Savolainen, 2017), a UWB-based method for mapping forest trees under a forest canopy was first introduced. However, an IMU sensor was required to correct the results, introducing complexity and unreliability over long distances and periods due to IMU drift. Furthermore, no exact measurement accuracy was provided in the patent, and thus, UWB remains an open-ended research topic for forest applications. In our study (Liu et al., 2024), we demonstrated that UWB technology could achieve decimetre-level localization accuracy with a root-mean-square-error (RMSE) of greater than 0.3 m under a forest canopy. We also highlighted the potential of UWB technology for other forest-related applications, such as locating foresters and robotics, as well as mapping forest trees under the forest canopy (Liu et al., 2025b, 2025a).

In this paper, we present a simple, low-cost, and reliable UWB-based method for mapping forest trees under the forest canopy, without the need for additional sensors or measurements. To our best knowledge, no previous studies have directly compared the performance of UWB and MLS for mapping forest trees under the forest canopy. Therefore, another goal of this paper is to compare the precision of the UWB method with that of MLS systems based on real-world datasets, aiming to provide a valuable reference for future forest-related studies.

This contribution has been peer-reviewed. The double-blind peer-review was conducted on the basis of the full paper.
https://doi.org/10.5194/isprs-annals-X-G-2025-551-2025

2. Material and Methods

2.1 Test Site

The test site used in this paper was located in the boreal forest zone near Evo, Finland (61.19°N, 25°11E), as part of the SCAN FOREST research infrastructure www.scanforest.fi. Given the limited coverage of the UWB system, approximately 80 m under the LoS conditions in open spaces, we selected a plot with an area of approximately 50 m × 110 m within this region to collect UWB data. The dominant tree species in this forest plot were Scots pine (*Pinus sylvestris*), with a small amount of Norway spruce (*Picea abies*) present. For the MLS data, a larger forest plot was tested, covering most of the area used for the UWB data collection. The MLS track spanned approximately 800 m in length, with a maximum displacement of 300 m from the starting location. The test site represents a typical managed forest in the boreal region of Finland, characterized by minimal understory vegetation and clear visibility, as described by Hyyppä et al. (2020b). As such, the test site was optimal for comparing the measurement accuracy of various methods for mapping forest trees. Figure 1 shows a photograph of the test site. Additionally, the average tree diameter at breast height (DBH) at the test site is approximately 0.3 m.

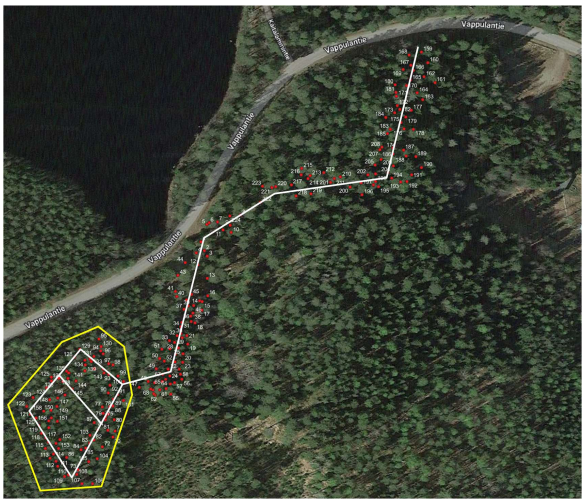

Figure 1. Overview of the forest environment. The solid yellow line represents the forest plot used for UWB data collection, while the solid white line indicates the approximate trajectory of the MLS device.

2.2 Data Collection Methods

2.2.1 UWB Data: All UWB devices used in this paper were based on the DW1000 chip from Decawave. Each device was integrated with a power amplifier and a low-noise amplifier to enhance coverage and improve receiver sensitivity. Table I provides the detailed parameters used by the UWB devices.

The UWB data was captured in May 2024 using six UWB beacons and one UWB terminal, as shown in Figure 2. The beacons were mounted on trees at a height of approximately 1.8 m from the ground using a custom-designed bracket. Their locations were automatically estimated by measuring the distances between them using a nonlinear least square method, as shown in Eq. 1. To enhance measurement accuracy, all the beacons were deployed as close to the same horizontal plane as possible. Additionally, to ensure reliable distance measurements for each pair of beacons within their coverage areas, each distance was measured 300 times. The median value of these measurements was then used as the final result, effectively reducing the impact of ranging outliers, especially when the dataset is small.

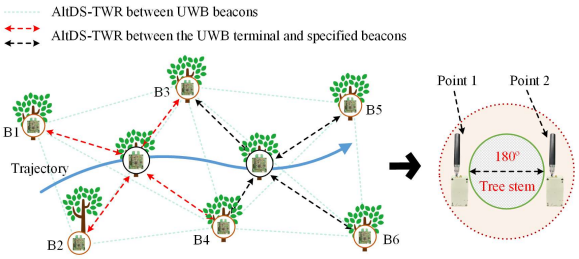

Figure 2. Overview of the data collection process of the UWB-based method. The centre of the tree trunk was defined as the tree’s position.

Table I. Configuration of the DW1000 chip.

Parameter	Channel	f_c	PRF*	Preamble	Data rate
value	2	4 GHz	64 MHz	512	110 kbps

*PRF denotes the pulse repetition frequency.

A forester held the terminal and moved around the test site at a speed of 1.5-2.5 m/s, stopping at each tree stem that needed to be mapped to collect raw distance measurements between the UWB terminal and beacons. The ranging rate was set to 10 Hz. To mitigate the effect of the random clock drifts of the devices on ranging accuracy and precision, the alternative double-side two-way ranging (AltDS-TWR) algorithm, proposed by Neirynck et al. (2017), was used for all distance measurements. AltDS-TWR offers more accurate ranging measurements with an overall RMSE of less than 2 cm under LoS conditions, compared to the traditional single-side TWR algorithm, which has an overall RMSE of approximately 5 cm. Additionally, to avoid duplicate or missing measurements, each tree to be mapped was labeled.

For each tree stem, two test points were measured close to the tree stem at approximately opposite angles (180 degrees apart) to improve measurement accuracy. The timestamps for when the measurement started and stopped for each tree stem were marked by pressing a button integrated with the terminal. The data collection time for each point was approximately 10 to 15 seconds. Finally, all data were transmitted to a smartphone via Bluetooth for post-processing.

2.2.2 MLS Data: Three commercial scanners, namely Zeb Horizon (GeoSLAM, UK), Hovermap (Emesent, Australia), and Deep Forestry (Deep Forestry, Sweden), were compared in this study. Deep Forestry and Hovermap were mounted on a drone flying under the forest canopy, while Zeb Horizon was a hand-held device. Hovermap and Zeb Horizon both utilized a rotating Velodyne VLP-16 laser scanner. Hovermap data was collected in September 2021 by AMKVO (Sweden) under our supervision, while Zeb Horizon data was collected in June 2021. Deep Forestry employed an Ouster OS0-32 Rev. 5 laser sensor, with data captured in September 2022 by Deep Forestry under our supervision. The Ouster OS0-32 had a beam width of 5 mm at the exit and a divergence of 6.1 mrad, whereas the Velodyne VLP-16 had a beam width of 9.5 (12.7) mm and a divergence of 1.5 (3.0) mrad vertically (horizontally).

In addition, only Hovermap was integrated with both GNSS and IMU sensors, while others relied solely on an IMU sensor. All

these systems relied on a SLAM algorithm of a certain version in order to correct the drifts of the IMU sensor. To collect the data in the same area in the test site for all the MLS systems, a similar 800 m-long track with a maximum displacement of approximately 300 m from the starting location in the test site was employed for all systems, as shown in Figure 1. The elevation change of the track is approximately 11 m, as demonstrated in (Muhojoki et al., 2024).

2.3 Tree Stem Location Extraction

2.3.1 UWB: To extract the tree stem locations, we first estimated the trajectory of the UWB terminal during the measurement. Specifically, we set the coordinates of *B1* to (0,0,0). Then, without the loss of generality, the LoS between *B1* and *B2* was used to define the x-axis. As a result, *B2* was assigned to the coordinates (d_{12},0,0), where d_{12} is the distance between *B1* and *B2*. A local coordinate system was used in this approach, where absolute positions were not essential. All other beacons were positioned in the positive x- and y-directions. Consequently, the coordinates of *B3* and *B4* could be determined only based on the measured distances between beacons *B1*, *B2*, *B3,* and *B4* by solving a nonlinear least-square problem with the following residuals:

$$\min \sum \left(\left\| \boldsymbol{l}_i - \boldsymbol{l}_j \right\|_2 - d_{ij} \right)^2 \tag{1}$$

where $\boldsymbol{l}_i$ = *i*-th position in the assumed coordinate system
d_{ij} = distance measurement between anchors *i* and *j*
$\left\| \bullet \right\|_2$ = Euclidean distance

The optimal solution of $\boldsymbol{l}_i$ was determined by minimizing the sum of the squared residuals. Afterward, the coordinates of *B5* and *B6* were calculated based on the measured distances between beacons *B3*, *B4*, *B5,* and *B6* using the same method. The trajectory of the kinematic terminal during the measurement was then estimated using the extended Kalman filter (EKF). Subsequently, location points corresponding to each tree stem measurement were extracted from the estimated trajectory, based on the recorded timestamps that marked the start and stop of each measurement. Finally, the optimal location estimates for the tree stems were obtained by averaging these location points.

For the collected data, some location points contained larger errors due to serious non-line of sight (NLoS) conditions during certain tree measurements. This led to significant errors in extracting the final tree stem locations. To address this issue, an efficient filter was developed to exclude these inaccurate location points for each tree measurement. This filtering was based on the density of the location points, where points exceeding a fixed threshold were classified as erroneous. These points are specifically expressed as,

$$\boldsymbol{x}_i = \{ \boldsymbol{X} \left\| h_i \right\| \geq \delta \in \boldsymbol{Y} \} \tag{2}$$

where $\boldsymbol{x}_i$ = filtered location points
h_i = obtained density of the *i*-th point
δ = specified threshold in the filter
$\boldsymbol{X}$ = reserved sets of the location points
$\boldsymbol{Y}$ = raw sets of the location points

Specifically, the density of each location point for each tree stem was determined by calculating the number of location points within a fixed radius. This can be expressed as,

$$h_i = Number\ of\ \{ \boldsymbol{Z} \left\| \boldsymbol{p}_i - \boldsymbol{Y} \right\|_2 < R \} \tag{3}$$

where $\boldsymbol{p}_i$ = location of the *i*-th point
R = specified search radius

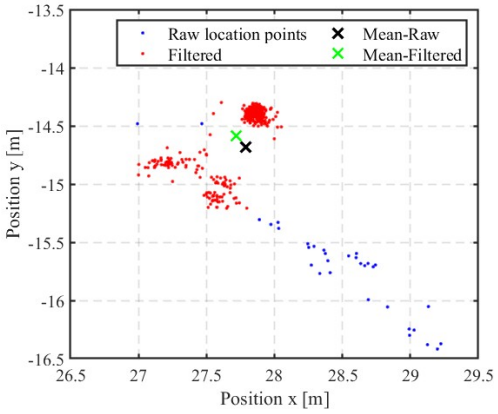

Figure 3. Comparison of the location points with and without the developed filter method. The blue dots represent the raw location points obtained by the positioning engine, while the red dots represent the filtered data based on Eq. (2) and Eq. (3).

Figure 3 shows an example of the obtained location points, where the parameters of δ and R are set to 30 and 0.4 m, respectively. It can be observed that some location points, which have larger location errors, are included in the example. These points are located far from the centre of the other points, with distances greater than 0.5 m, as highlighted in blue. Without any filtering, these points could introduce significant errors in the final estimation of the tree stem location, as shown in Figure 3 and highlighted by the black fork.

2.3.2 MLS: First, stem curves were extracted from the MLS data using the algorithm demonstrated in (Hyyppä et al., 2020a). Then, the tree stem locations were determined at the height of 1.3 m using the extracted stem curve and the algorithm demonstrated in (Muhojoki et al., 2024).

In the tree stem extraction process, point clouds were first segmented spatially and temporally. The arcs corresponding to hits on the tree trunks were then extracted. To obtain stem radii at different heights, the growth direction of the tree was calculated using the principal component analysis (PCA). Circles were then fitted to the arcs along the calculated growth direction. Some of the obtained stem radii were rejected if the arcs did not meet the quality criteria, which were based on the central angle and the amount of noise points. Finally, the tree stem curve was created by fitting a smoothing spline to the radii. As mentioned by the authors, the algorithm was designed for trees with nearly vertical stems in relatively sparse forests (Hyyppä et al., 2020a).

In the tree stem estimation process, a novel ground estimation method was further developed to improve the horizontal position estimate of the tree stem if the tree was tilted, and at the same time to eliminate the trees where the surrounding ground was poorly visible, as demonstrated by Muhojoki et al. (2024). First, all the point clouds within 15 cm of the initial digital terrain model (DTM) were classified as ground points. The tree location at ground level was then calculated using the learning direction by the PCA. To prevent any stem points from being classified as ground, all ground points within a maximum radius of the tree +10 cm from that location were removed. Additionally, distant

points were discarded, leaving a ring of points with a thickness of 40 cm, as outlined by Muhojoki et al. (2024). To account for the influence of rocks and roots on the forest floor, a kernel density estimation (KDE) using a normal distribution kernel and adaptive bandwidth was applied to smooth the distribution of the remaining ground points. The mode of the density estimate was then used as the renewed ground estimation. Any trees with fewer than 50 points in the ground estimation were discarded. Finally, the tree stem locations at the height of 1.3 m were re-calculated.

All data from the three commercial MLSs were processed using the same algorithms and parameters, as demonstrated in (Hyyppä et al., 2020a) and (Muhojoki et al., 2024) .

2.4 Field Reference

The field reference was obtained using a high-density airborne laser scanning (ALS) integrated with a helicopter, referred to as HeliALS-TW. This system was developed in the office and integrated with a Riegl VUX-1HA scanner, a NovAtel ISA-100C inertial measurement unit, a NovAtel PwrPak 7 GNSS receiver, and a NovAtel GNSS-805 antenna. The helicopter flew at an altitude of approximately 80 m above ground level at a speed of approximately 9.5 m/s in a grid pattern, with vertical lines spaced 50 m. According to the Riegl VUX-1HA production datasheet, the scanner's divergence was 0.5 mrad, and the laser beam footprint was 4.5 mm at exit, increasing to 50 mm at a distance of 100 m. To maximize the likelihood of the laser beams hitting the tree stems and thereby improve measurement accuracy, the scanner was tilted 15˚ forward relative to the vertical plane. The average return point density was 1844 points per square meter.

Additionally, the trajectory of the HeliALS-TW was estimated using Waypoint Inertial Explorer (version 8.9, NovAtel Inc., Canada) and a single virtual GNSS-based station from Trimnet VRS service (RINEX 3.04), which was located approximately in the middle of the test site. Finally, the tree stem locations were extracted from the point clouds using the tree stem extraction algorithm proposed by Hyyppä et al. (2020b).

According to the results from Muhojoki et al. (2024), the RMSE and MAE of HeliALS-TW were 6.12 cm and 4.86 cm, respectively, in the horizontal direction, and 8.03 cm and 10.32 cm in the vertical direction, when compared with the field reference data obtained by the total station. It should be noted that the HeliALS-TW data included more reference trees (188) than the total station data (89) for the tested forest plot. Consequently, in this paper, only the tree stem locations derived from the HeliALS-TW data and the tree trunk extraction approach proposed by Hyyppä et al. (2020b) were used as the field reference to estimate the accuracy of other field tests.

2.5 Georeferencing

Based on the method demonstrated by Muhojoki et al. (2024) for comparing the positioning accuracy of different mobile laser scanner systems, data can be georeferenced by registering the tree locations obtained from the new method to the field reference using the 2D registration algorithm proposed by Hyyppä et al. (2021). This process allows for evaluating the measurement accuracy of tree mapping for the new method. The algorithm includes two registration steps: a coarse 2D registration to identify matching tree pairs and a fine registration that optimizes the tree locations using the iterative closest point (ICP) algorithm (Besl and McKay, 1992). By adjusting the parameters, such as the search radius, the number of tentative matches, and the registration threshold, the trees from different datasets are registered as matching tree pairs. However, it is important to note that a too-small registration threshold will result in fewer matching tree pairs, while a threshold that is too large will cause errors or duplications in the registration of the same tree. In this paper, we used a search radius of 5 m and a registration threshold of 60 cm in the 2D registration algorithm, meaning that only trees within 60 cm of a reference tree location after the optimal transformation are registered as a matching tree pair. The Matlab functions of the 2D registration algorithm are available from a public repository (Hyyppä and Muhojoki, 2021).

2.6 Evaluation Metrics

We evaluated the accuracy of the tested methods based solely on the horizontal tree stem locations in the OXY plane, as only 2D tree stem locations were obtained for UWB. As is typical, tree stem locations in the OXY plane are considered more important than those in the OXZ/OYZ plane. Furthermore, the methods were compared based on precision rather than global accuracy due to the absence of GNSS data for the UWB. In the precision category, systematic errors were eliminated from the tree locations, assuming the reference was accurate, while these errors remained in the evaluation of global accuracy based on the field reference used.

Although no GNSS receiver data were included for UWB, the OXY plane fitting method, described in Section 2.5, was still implemented as a part of the georeferencing process to acquire the matching trees. The precision of the tree stem locations for the tested methods was then compared using the RMSE and mean-absolute-error (MAE):

$$RMSE = \sqrt{\frac{1}{N_{\boldsymbol{M}}} \sum_{i \in \boldsymbol{M}} \left\| \boldsymbol{p}_i - \boldsymbol{p}_{ref,i} \right\|_2^2} \tag{4}$$

$$MAE = \frac{1}{N_{\boldsymbol{M}}} \sum_{i \in \boldsymbol{M}} \left\| \boldsymbol{p}_i - \boldsymbol{p}_{ref,i} \right\|_2 \tag{5}$$

where $\boldsymbol{M}$ = set of matched trees
$N_{\boldsymbol{M}}$ = number of the matched trees
$\left\| \boldsymbol{p}_i - \boldsymbol{p}_{ref,i} \right\|_2$ = Euclidean distance
$\boldsymbol{p}_i$ = coordinate of a matched tree stem
$\boldsymbol{p}_{ref,i}$ = coordinate of the corresponding reference tree

3. Results and Discussion

Figure 4 shows the registration results obtained using HeliALS data as the field reference. Note that the locations of the trees extracted from the UWB and MLSs have been shifted so that the average location is approximately zero in both the x and y directions for clarity. However, comparing the precision of the tested methods is not the focus here.

For the UWB, 349 trees were mapped in the test site, with 160 trees registered as matching tree pairs. For the MLSs, 243, 678, and 424 trees were mapped in the test site, with 183, 319, and 288 trees registered as matching tree pairs for Deep Forestry, Hovermap, and Zeb Horizon, respectively. Since the number of the mapped and registered trees for the UWB and Deep Forestry are significantly lower than those of the Hovermap and Zeb Horizon, the comparison was performed using only the registered trees within nearly the same forest plot, the area to the left of the dotted green line, as shown in Figure 4. In this area, 160, 146, 178, and 158 trees were registered as matching tree pairs for UWB, Deep Forestry, Hovermap, and Zeb Horizon, respectively.

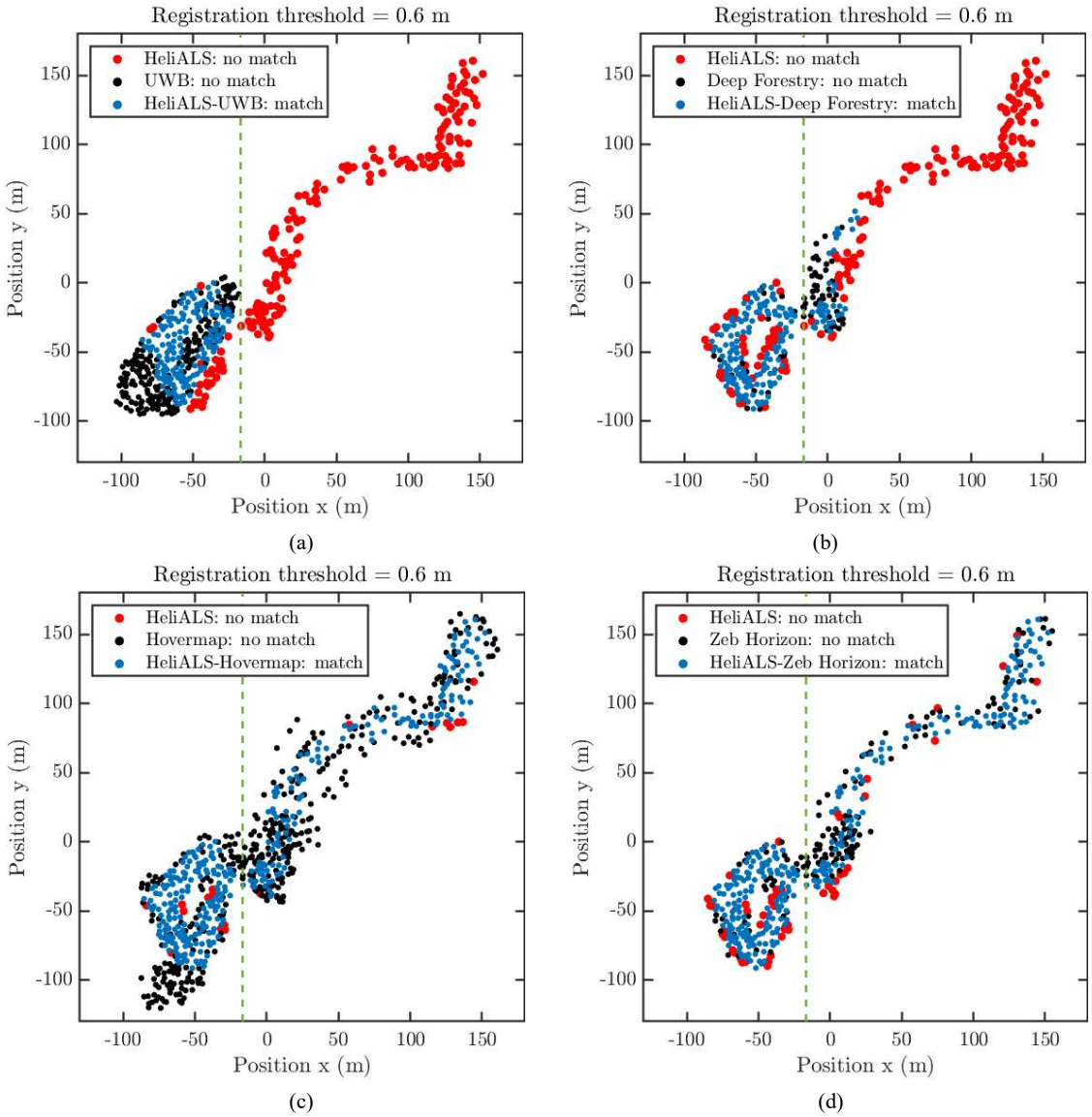

Figure 4. Tree maps of UWB and MLSs registered to the HeliALS trees. (a) results of the UWB data-driven method, and (b) to (d) results of three commercial MLSs. The red and black dots represent the locations of trees detected from the HeiliALS data and other field tests without a matching tree pair in the tested data, while the blue dots show the locations of trees extracted from the tested data with a matching tree pair. The coordinates are centered around the mean HeliALS tree location for clarity.

The statistical results are presented in Figure 5 and Table II. In addition to RMSE and MAE, Table II also includes the statistical results for the maximum and minimum errors (MAX and MIN), standard deviation (STD), and the 68% and 95% errors in the cumulative distribution functions (CDF), as well as the time required to take all tree positions for both UWB and MLSs.

Based on the aligned tree maps, the UWB system was able to achieve accurate measurements for tree stem locations under the forest canopy with an RMSE of 14.44 cm and a MAE of 12.39 cm, providing accuracy comparable to that of the three tested commercial MLSs. The 95% error in the CDF of the UWB is approximately twice that of the three MLSs, while the 68% error in the CDF of the UWB is similar to the three MLSs.

For UWB, the precision is mainly affected by the estimated local coordinates of the beacons in the test site and by the NLoS measurements between the terminal and beacons. Both factors introduce positioning errors in the trajectory and, consequently, in the tree stem locations. To cover as much of the forest as possible, the beacons were placed at the corners of the environment, resulting in NLoS conditions between them. To facilitate tree mapping, the UWB terminal was placed as close as possible to the tree stem during measurements, leading to significant NLoS conditions between the terminal and beacons.

In addition, for UWB, setting up the network with enough beacons (e.g., six) takes less than 30 minutes for a single-person team, including placing the beacons on trees and collecting the distances between them. Then, for each tree to be mapped, data were captured in approximately 20 to 30 seconds. Therefore, for a forest with 100 trees, the total time required for the UWB to collect all the data will be approximately one and a half hours, excluding other tasks during the measurements. Furthermore, UWB data post-processing can be completed in half an hour. Based on our experience, a portable SLAM laser scanner takes

approximately half an hour to collect all the data in the same forest plot. However, data post-processing is usually time-consuming and depends on dataset size and algorithm complexity. Typically, it takes one to two hours to obtain the final locations of all the trees from the point clouds.

Furthermore, although the UWB system is inexpensive, usually less than one hundred euros per device, it is more challenging to cover a larger forest area under the canopy compared to the MLS, due to the device’s limited coverage. Additionally, mapping forest trees in 3D is more difficult for UWB because of the unknown relative height of the beacons in the vertical direction. Moreover, UWB typically operates under the forest canopy, enabling it to function even in deep forests with fully closed canopies.

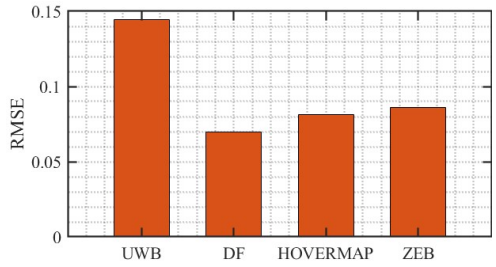

(a) RMSE

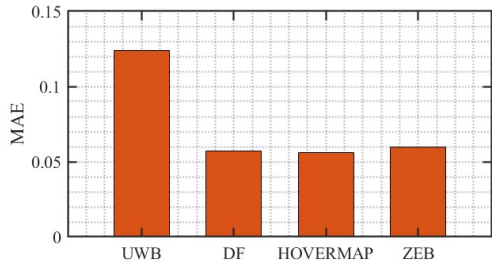

(b) MSE

Figure 5. Precision of UWB and MLSs in the horizontal direction in the specified forest plots.

Table II. Statistical results on the precision and time required to take all the positions for the compared methods, unit [cm].

Method	UWB	Deep Forestry	Hovermap	Zeb Horizon
RMSE	**14.44**	**5.70**	**5.61**	**5.98**
MAE	**12.39**	**6.98**	**8.11**	**8.58**
MAX	37.80	17.23	36.70	30.29
MIN	1.28	0.34	1.91	1.62
STD	7.46	3.19	4.03	3.92
68%	13.98	8.35	11.80	12.44
95%	27.46	12.50	14.99	17.23
Tree pairs	160	146	178	158
Time [h]	< 3.5	< 2.5	< 2.5	< 2.5

4. Conclusion

In this study, we present a UWB-based method for mapping forest trees under a forest canopy with reduced human efforts, without the need for any other sensors or measurements. We compare its precision with that of three commercial MLSs using real-world datasets. The experimental results demonstrate that the UWB-based method can achieve decimetre-level (< 0.15 m) accuracy in mapping forest trees under the forest canopy, compared to ALS-based field reference, providing accuracy comparable to that of the three tested MLSs. Additionally, UWB is significantly cheaper than the commercial MLSs, making it an optional solution not only for academia but also for industry, facilitating forest surveying and management. Future research should focus on additional comparisons across different forest sites with varying tree densities.

Acknowledgments

This work was supported by funds granted by the Research Council of Finland through the UNITE Flagship (359175), projects ‘Capturing structural and functional diversity of trees and tree communities for supporting sustainable use of forests / Consortium: Diversity4Forests’ (338644), ‘High-performance computing allowing high-accuracy country-level individual tree carbon sink and biodiversity mapping (359203)’ and ‘Feasibility of Inside-canopy UAV laser scanning for automated tree quality surveying / Consortium: Quality4Trees’ (334002), and by the Ministry of Agriculture and Forestry of Finland and European Union NextGenerationEU through the project IlmoStar (VN/27353/2022). The tests were done at ScanForest research infrastructure supported by the Research Council of Finland (346382).

We are grateful to Jesse Muhojoki for providing the tree stem locations obtained by the three commercial MLSs and HeliALS-TW, and to Eric Hyyppä and Jesse Muhojoki for providing the code (Hyyppä and Muhojoki 2021) of the 2D-registration method demonstrated in (Hyyppä et al. 2021).

References

Besl, P.J., McKay, N.D., 1992. A method for registration of 3-D shapes. IEEE Transactions on Pattern Analysis and Machine Intelligence, 14, 239–256.

Edson, C., Wing, M.G., 2012. Tree location measurement accuracy with a mapping-grade GPS receiver under the forest canopy. Forest Science, 58, 567–576.

Holopainen, M., Kankare, V., Vastaranta, M., Liang, X., Lin, Y., Vaaja, M., Yu, X., Hyyppä, J., Hyyppä, H., Kaartinen, H., Kukko, A., Tanhuanpää, T., Alho, P., 2013. Tree mapping using airborne, terrestrial and mobile laser scanning - A case study in a heterogeneous urban forest. Urban For Urban Green, 12, 546–553.

Hyyppä, E., Hyyppä, J., Hakala, T., Kukko, A., Wulder, M.A., White, J.C., Pyörälä, J., Yu, X., Wang, Y., Virtanen, J.P., Pohjavirta, O., Liang, X., Holopainen, M., Kaartinen, H., 2020a. Under-canopy UAV laser scanning for accurate forest field measurements. ISPRS Journal of Photogrammetry and Remote Sensing, 164, 41–60.

Hyyppä, E., Kukko, A., Kaijaluoto, R., White, J.C., Wulder, M.A., Pyörälä, J., Liang, X., Yu, X., Wang, Y., Kaartinen, H., Virtanen, J.P., Hyyppä, J., 2020b. Accurate derivation of stem curve and volume using backpack mobile laser scanning. ISPRS Journal of Photogrammetry and Remote Sensing, 161, 246–262.

Hyyppä, E., Muhojoki, J., 2021. 2d-registration. https://gitlab.com/fgi_nls/public/2d-registration.

Hyyppä, E., Muhojoki, J., Yu, X., Kukko, A., Kaartinen, H., Hyyppä, J., 2021. Efficient coarse registration method using translation- and rotation-invariant local descriptors towards fully automated forest inventory. ISPRS Open Journal of Photogrammetry and Remote Sensing, 2, 100007.

Kukko, A., Kaijaluoto, R., Kaartinen, H., Lehtola, V. V., Jaakkola, A., Hyyppä, J., 2017. Graph SLAM correction for single scanner MLS forest data under boreal forest canopy. ISPRS Journal of Photogrammetry and Remote Sensing, 132, 199–209.

Liang, X., Kukko, A., Balenovic, I., Saarinen, N., Junttila, S., Kankare, V., Holopainen, M., Mokros, M., Surovy, P., Kaartinen, H., Jurjevic, L., Honkavaara, E., Nasi, R., Liu, J., Hollaus, M., Tian, J., Yu, X., Pan, J., Cai, S., Virtanen, J.P., Wang, Y., Hyyppa, J., 2022. Close-range remote sensing of forests: The state of the art, challenges, and opportunities for systems and data acquisitions. IEEE Geoscience and Remote Sensing Magazine, 10, 32–71.

Liang, X., Kukko, A., Hyyppä, J., Lehtomäki, M., Pyörälä, J., Yu, X., Kaartinen, H., Jaakkola, A., Wang, Y., 2018. In-situ measurements from mobile platforms: An emerging approach to address the old challenges associated with forest inventories. ISPRS Journal of Photogrammetry and Remote Sensing, 143, 97–107.

Liu, Z., Kaartinen, H., Hakala, T., Hyyppa, J., Kukko, A., Chen, R., 2024. Performance analysis of standalone UWB positioning inside forest canopy. IEEE Transactions on Instrumentation and Measurement, 73.

Liu, Z., Kaartinen, H., Hakala, T., Hyyppä, J., Kukko, A., Chen, R., 2025a. Tracking foresters and mapping tree stem locations with decimeter-level accuracy under forest canopies using UWB. Expert Systems with Applications, 262.

Liu, Z., Kaartinen, H., Hakala, T., Hyyti, H., Hyyppa, J., Kukko, A., Chen, R., Vastaranta, M., 2025b. Ultra-Wideband-Based Method for Measuring Tree Positions with Decimeter-Level Accuracy Under a Forest Canopy. IEEE Journal of Selected Topics in Applied Earth Observations and Remote Sensing, 18, 12961-12972.

Muhojoki, J., Hakala, T., Kukko, A., Kaartinen, H., Hyyppä, J., 2024. Comparing positioning accuracy of mobile laser scanning systems under a forest canopy. Science of Remote Sensing, 9.

Neirynck, D., Luk, E., McLaughlin, M., 2017. An alternative double-sided two-way ranging method, in: *Proceedings of the 2016 13th Workshop on Positioning, Navigation and Communication, WPNC 2*016. Institute of Electrical and Electronics Engineers Inc.

Pekka Savolainen, 2017. Method for positioning and measuring trees on a sample plot.

Stovall, A.E.L., MacFarlane, D.W., Crawford, D., Jovanovic, T., Frank, J., Brack, C., 2023. Comparing mobile and terrestrial laser scanning for measuring and modelling tree stem taper. Forestry, 96, 705–717.